Biaxial strength and slow crack growth ~~of~~ in porous alumina with silica sintering aid

Astrid Bakken[a,*], Susanne Wagner[b], Michael J. Hoffmann[b], Bernt Thorstensen[c], Mari-Ann Einarsrud[a], Tor Grande[a]

[a]*Department of Materials Science and Engineering, Norwegian University of Science and Technology, NO-7491 Trondheim, Norway*
[b]*Institute for Applied Materials-Ceramics in Mechanical Engineering, Karlsruhe Institute for Technology (KIT), D-76131 Karlsruhe, Germany*
[c]*KeraNor AS, Brobekkveien 104 A, NO-0582 Oslo, Norway*

Abstract

Biaxial strength, fracture toughness and subcritical crack growth are reported for coarse grained porous alumina ceramics. The materials were prepared with a varying amount of a silica sintering aid, which resulted in the formation of a glassy secondary phase at the grain boundaries. Crystalline mullite was found in addition to the glass in the material with the highest silica content. The biaxial strength, measured both by Ball-on-Ring ~~(BOR)~~ and Ball-on-3-Balls (~~BO3B~~), was highest for the material without mullite at the grain boundaries, and the biaxial strength decreased with increasing porosity. The fracture toughness of the materials was in the range of 1.7-1.9 MPam$^{0.5}$. Measurements of subcritical crack growth by a modified lifetime method in air and aqueous environments demonstrated a higher crack growth rate in water and acid relative to in air. The effect of porosity and grain boundary phase were discussed in relation to subcritical crack growth and fracture mode in the coarse grained alumina ceramics. ~~The crack growth rate was slightly higher in the material with only a glass phase at the grain boundaries.~~

Keywords: Porous alumina, Biaxial strength, Fracture toughness, Subcritical crack growth

1. Introduction

Alumina ceramics are widely used today due to its excellent properties such as high hardness [1], chemical inertness [2, 3], thermal stability [4] and low electrical conductivity [5]. In most of these applications dense ceramics are desired, and MgO is mostly used as a sintering aid for sintering of high performance dense alumina ceramics [6–8]. Porous alumina ceramics on the other hand, where the porosity can be tailored by the use of pore forming agents or by using coarse grained powders, have also potential applications such as in filters, catalyst support and in membranes [9, 10]. In many of these applications the porous alumina material can be exposed to a mechanical load in various aqueous or chemical environments, which address the importance of understanding subcritical crack growth and fracture mode in the porous materials.

The mechanical permanence of alumina ceramics such as strength and fracture toughness have been studied extensively due to the technical importance of alumina ceramics [4, 11–13]. The mechanical performance depends on porosity, the presence of other phases at the grain boundaries and also humidity. Biaxial strength and effect of environment on the mechanical permanence of alumina-based ceramics have been measured on ceramic plates by Ball-on-Ball (BOB) or Ball-on-3-Balls (B3B) methods [14–16]. Subcritical crack growth (SCCG) may occur when cracks grow under an applied stress intensity factor, K_I, well below the fracture toughness, K_{IC} [17]. SCCG is related to presence of humidity in ceramics [11, 14, 18, 19]. Polar molecules, such as water, may interact with the strained crack tip, which will weaken the bond at the crack tip. With presence of humidity, SCCG may also influence the determination of fracture toughness as recently addressed by Krautgasser et al. and Quinn and Swab for low-temperature co-fired ceramics and glasses, respectively [20, 21]. Though in case of high purity alumina with submicron grain size no effect of humidity has been reported [14]. In alumina ceramics fast fracture often propagates by a transgranular

*Corresponding author
Email address: astrid.bakken@gmail.com (Astrid Bakken)

mode, whereas slow crack growth propagates by intragranular mode, especially for materials with finer grain size [18, 22]. However, the fracture mode depends on the strength and the phases present at interfaces in the material. ~~The biaxial strength of dense and high purity Al_2O_3 obtained by the Ball-on-3-Balls (B3B) technique have been reported in the range 380-470 MPa [15]. Similar biaxial strength values were obtained by the 4-point bending test [4]. Subcritical crack growth in polycrystalline alumina have been reported down to 10^{-13} [m/s](K_I=3.1 MPam$^{0.5}$) and crack growth exponents have been reported between n=31 and 52 in different environments [14][17][11][12][18]. The presence of water vapor or water promotes subcritical crack growth [11][18]. However, other authors report no effect of water in case of high purity and with submicron grain size [14].~~

In this work we report on biaxial strength and subcritical crack growth of three porous alumina ceramics prepared by using coarse grained alumina powder and silica as sintering aid. Biaxial strength was measured by both the B3B and BOR methods. The subcritical crack growth was measured by the modified lifetime method [23] in three different media. The biaxial strength and subcritical crack growth is discussed with respect to the grain boundary phases, fracture mode and open porosity of the materials.

2. Experimental

Material specifications

The porous alumina ceramic plates were fabricated by KeraNor AS. Dry and wet binder, plasticizer, dispersant and a colloidal suspension of silica was added to coarse alumina powder (Almatis T60, $Na_2O \leq 0.4\%$). This was mixed in a high speed Eirich mixer, and then homogenized and rolled down to a thickness of 1 mm. The plates were cut into circular specimens of 20 mm(ø) and square 30x30 mm^2. Material A, B and C contain 2.7, 4.0 and 4.8 wt% silica respectively, Table 1. Material A and B were sintered at 1700 °C and material C was sintered at 1650 °C.

Characterization

Biaxial strength was determined by both Ball-on-3-Balls (B3B) and Ball-on-Ring (BOR) technique with a loading rate of 1.0 mm/min [24, 25]. Three balls with diameter of 10 mm were placed in a cylinder with an inner diameter of 22 mm. The specimen (d=20 mm, t=1 mm) was placed between the three touching balls and a fourth ball, which was kept in central position of the specimen by a supporting lid with centered hole. In the BOR setup the specimen (30x30 mm^2, t=1 mm) was placed between a circular support ring (d=20 mm) and a load ring where the ball (d=0.5 mm) was placed. Lifetime of the specimens was determined in the B3B test by applying a constant load, where time until final failure was recorded. The applied load of 181 MPa (material A) and 136 MPa (material C) corresponds for both materials to a fracture probability of 0.6%. The time for a specimen to be a survivor was set to 20000 s. Lifetime measurements were performed in ambient air, water and sulphuric acid (H_2SO_4, 0.1 M). All the tests were started immediately after immersion in the liquid. The data were ranged according to the Weibull distribution [26].

Subcritical crack growth was determined by using the modified lifetime method by Munz and Fett [23], relating inert bending strength and lifetime measurements. The crack growth rate v(K_{Ii}) is given by Eq. 1.

$$v(K_{Ii}) = -\frac{2}{t_{Bi}\sigma_{ci}^2}\left(\frac{K_{IC}}{Y}\right)^2 \frac{d\left[log\left(\frac{\sigma_a}{\sigma_{ci}}\right)\right]}{d\left[log(t_{Bi}\sigma_a^2 Y^2)\right]} \quad (1)$$

where σ_a is the static load level, σ_{ci} is the inert strength, Y is the geometrical factor (circular=1.33), t_{Bi} is the lifetime and K_{IC} is the fracture toughness. The last term in Eq. 1 is found by linear regression of logarithmic plot of σ_a/σ_{ci} versus $t_{Bi}\sigma_a^2 Y^2$.

The fracture toughness (K_{IC}) was determined with the Single-Edge-Notched-Beam (SENB) technique [27]. The test was performed with a four-point-bending setup on five specimens with dimensions 3×4×50 mm^3. The specimens were prenotched by using a razor blade notch lapping machine together with diamond paste of 15,3 and 1 µm. In this way a crack tip radii of < 8 µm could be realized, which is considerably lower than the average grain size of the starting material.

Investigation of the microstructure and the chemical composition of the materials was performed with scanning electron microscope (SEM, Hitatchi S-3500N) with Energy Dispersive Spectrometry (EDS). Density measurements were performed by using Archimedes method in 2-propanol according to the international standard ISO 5017. X-ray

diffraction (XRD) was used to determine presence of crystalline secondary phases by using Bruker AXS D8 FOCUS diffractometer with CuKα radiation.

3. Results

The microstructure of the three materials is shown in Fig. 1. In Table 1 the amount of silica sintering aid, rela-

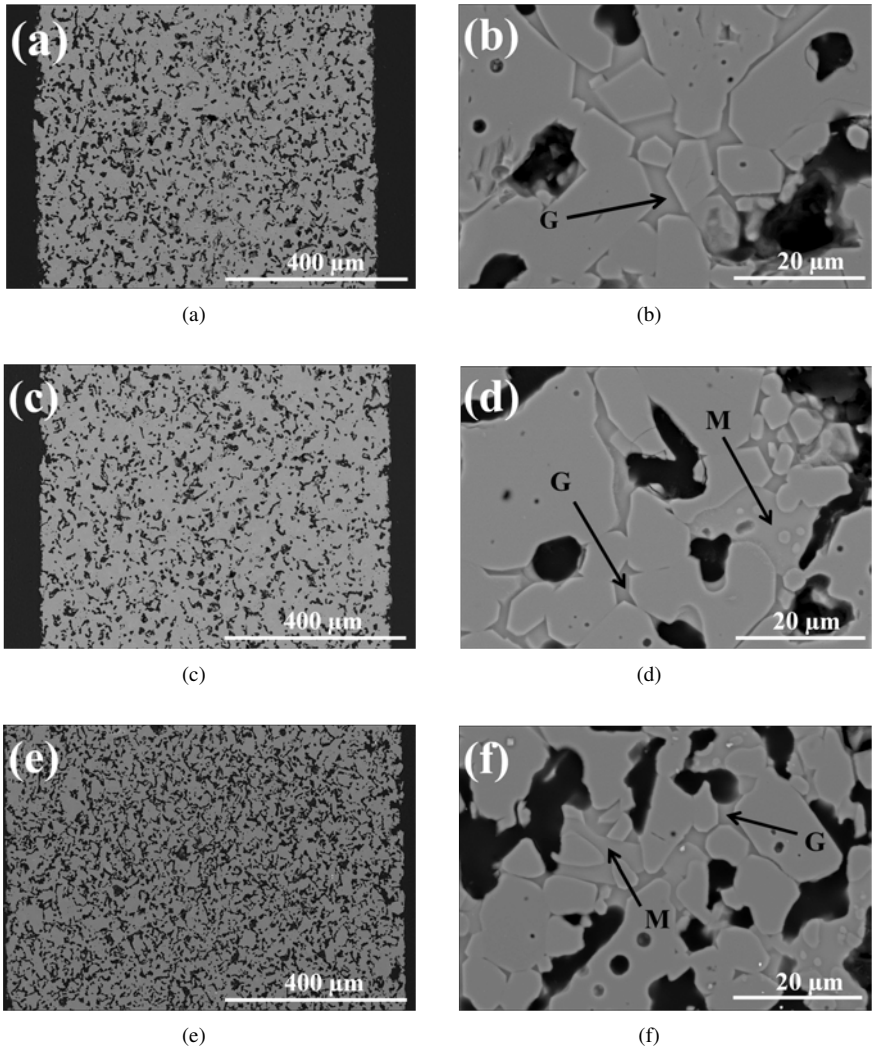

Figure 1: Microstructure of material A (a)-(b), B (c)-(d) and C (e)-(f) at low and high magnification. The presence of mullite was identified with EDS and XRD. Mullite is marked with M and the glassy sodium aluminosilicate phase with G.

tive density and open porosity are summarized. The materials are relatively homogeneous with large alumina grains separated by smaller open pores with a grain boundary phase binding the coarse alumina grains together. A sodium aluminosilicate amorphous phase was found at the grain boundaries by SEM/EDS. The two materials with the highest silica content contained also crystalline mullite as shown by the XRD patterns in Fig. 2 and identified by SEM/EDS in Fig. 1. The amorphous phase is most likely a glass formed during cooling of a liquid phase with the same composition [28]. There is low contrast between the mullite and the glassy sodium aluminosilicate phase. The sodium aluminosilicate glass gives a higher contrast with a distinct interface towards the alumina grains than observed towards mullite. Sections with mullite are often larger and appear as grains, compared to the the glassy phase. The contrast

Table 1: The nominal silica content , density, open porosity and observed secondary phases for the materials used in this study.

Material	***Silica*** *[wt%]*	***Density*** *[g/cm^3]*	***Density*** *[%]*	***Open porosity*** *[%]*	***Secondary phases***
A	2.6	3.0±0.02	75.6±0.4	21.0±0.3	glass
B	4.0	3.0±0.02	75.5±0.5	20.4±0.6	glass, mullite
C	4.8	2.7±0.04	67.3±0.8	28.9±0.7	glass, mullite

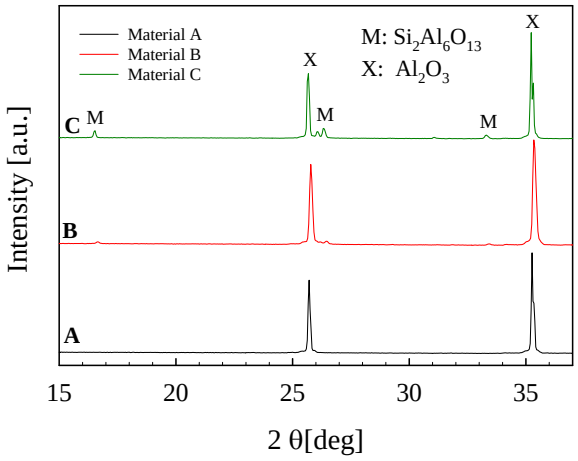

Figure 2: XRD pattern of the three alumina ceramics with identification peaks of Al_2O_3 (X) and mullite, $Al_6Si_2O_{13}$, (M).

Table 2: Biaxial strength, σ_o (±95% CI), and Weibull modulus, m, obtained by the BOR and the B3B technique, fracture toughness, K_{1C} (±SD), obtained by SENB testing and parameters from power law relation v=Ax^n of the crack velocities in Fig. 6.

	BOR		***B3B***			*Air*		*Water*		*Acid*	
Material	σ_o *[MPa]*	***m*** -	σ_o *[MPa]*	***m*** -	K_{1C} *[MPam$^{0.5}$]*	***A*** $\cdot 10^{-3}$ *[m/s]*	***n*** -	***A*** $\cdot 10^{-3}$ *[m/s]*	***n*** -	***A*** $\cdot 10^{-3}$ *[m/s]*	***n*** -
A	241±3	26	245±3	25	1.9±0.1	1.5	44	13	47	3.1	39
B	226±4	18	-	-	-	-	-	-	-	-	-
C	164±2	25	172±2	31	1.7±0.1	0.6	46	1.6	48	1.3	43

between the phases is more apparent from the EDS mapping of aluminium, silicon and sodium shown in Fig. 3. The

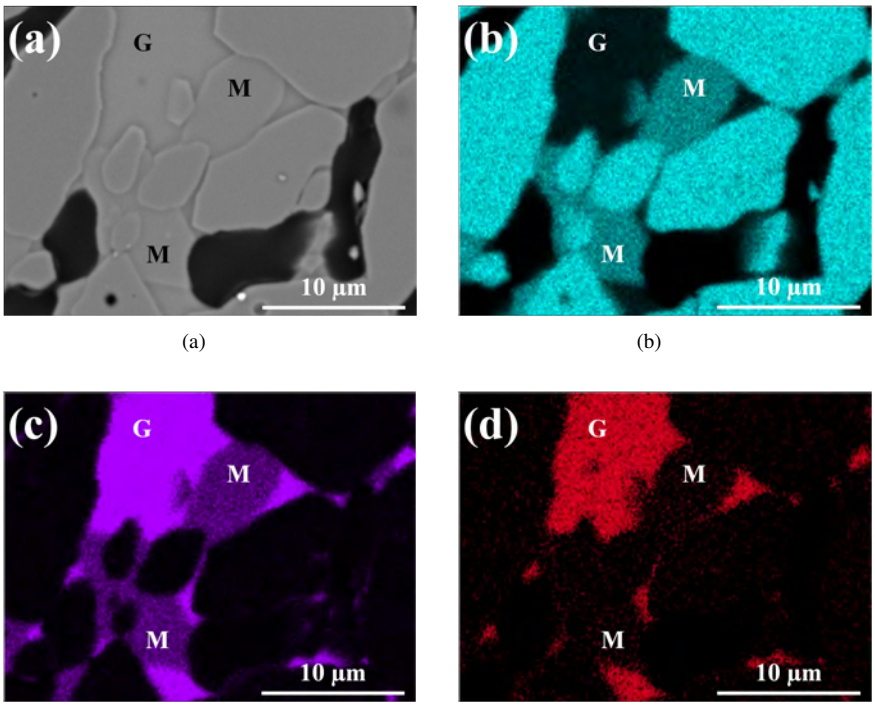

Figure 3: EDS mapping of material C from Fig. 1(f) at lower magnification (a) area selection (b) Al, (c) Si and (d) Na. Mullite is marked with M and the glassy sodium aluminosilicate phase with G.

glass is distributed between grains typical for materials prepared by liquid phase sintering and is ~~indicated~~ by high intensity of sodium and silicon. The mullite content was highest in the material with the highest silica content, which demonstrates that the phase composition, found after cooling to room temperature, reflects the phases present at the sintering temperature in line with the Na_2O-Al_2O_3-SiO_2 phase diagram [29].

The biaxial strength, determined by BOR and B3B, is shown in the Weibull distribution plots displayed in Fig. 4. The biaxial strength and the Weibull modulus obtained by the two techniques are summarized in Table 2. The high values of the Weibull modulus indicate a narrow defect distribution and consequently a relative low scattering of the measured fracture stresses. The biaxial strength measured by the BOR is comparable to the B3B measurements. Material C has significantly lower biaxial strength, reflecting the higher porosity of this material. The fracture toughness obtained by SEVNB performed with 4-point bending test was 1.9±0.1 MPam$^{0.5}$ and 1.7±0.1 MPam$^{0.5}$ of material A and C, respectively, (Table 2). The fracture toughness measured here is in good accord with a recent report by Norton et al. [13] for polycrystalline alumina. Although not specifically investigated by this study, SCCG may have influence

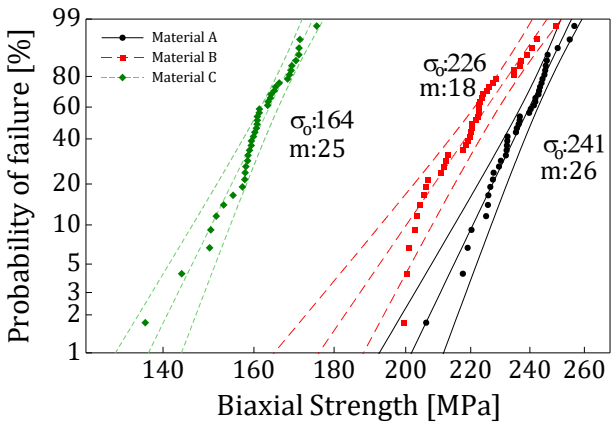

(a)

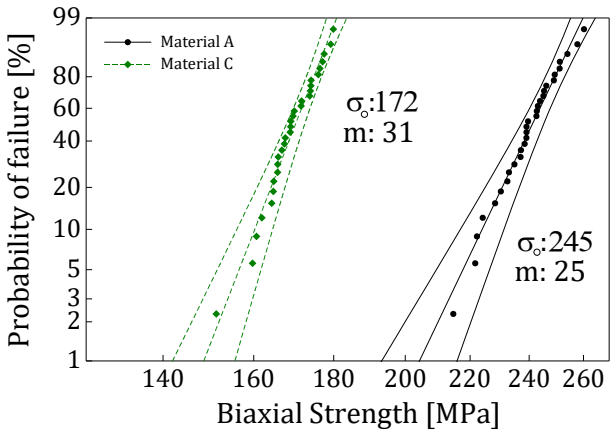

(b)

Figure 4: Weibull distribution of the biaxial strength obtained by (a) BOR of material A, B and C and by (b) B3B of material A and C. The middle lines represent the best distribution fit of the data while the outermost lines represent the 95% confidence interval.

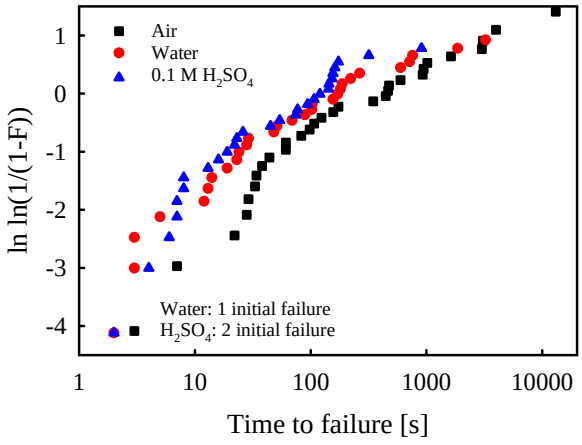

(a)

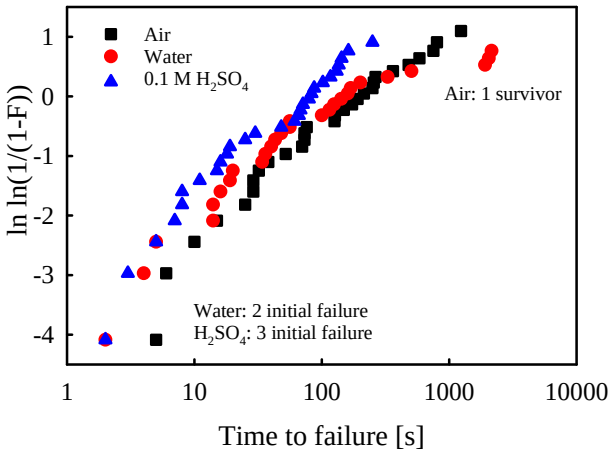

(b)

Figure 5: Weibull distribution of the lifetime measurements with B3B with constant load of material A (a) and C (b) in air, water and 0.1 M H_2SO_4.

on the determination of the fracture toughness as discussed by Krautgasser et al. [20].

The lifetime measurements from the B3B test with constant load in air, water and acid are given for material A and C, in Fig. 5. As expected, the lifetime of the specimens in the two aqueous environments are lower than in air for both materials. In material A spontaneous failure (at zero time) occurred of one specimen in water and two in acid. For material C, two specimens failed spontaneously in water and three in acid. One specimen of material C (air) did not fail before reaching the time limit, hence it was a survivor.

The crack growth rates of material A and C are shown in Fig. 6. A lower subcritical crack growth rate can be observed in experiments performed in air compared to aqueous environments of both materials. Furthermore, a higher crack growth rate was observed for material A relative to material C in air, water and acid. The crack growth rate (v) for static loading as a function of the K_I/K_{IC} ratio can be fitted by the following power law, Eq. 2.

$$v = \frac{da}{dt} = A^* \left(\frac{K_I}{K_{IC}} \right)^n \tag{2}$$

The parameters n and A^* from the power law fitting of the subcritical crack growth are given in Table 2. The stress exponents of material A and C were similar. In the case of measurements in water, six specimens of material C deviated from the power law approximation. Including all the specimens gave a high crack exponent of 62, whereas

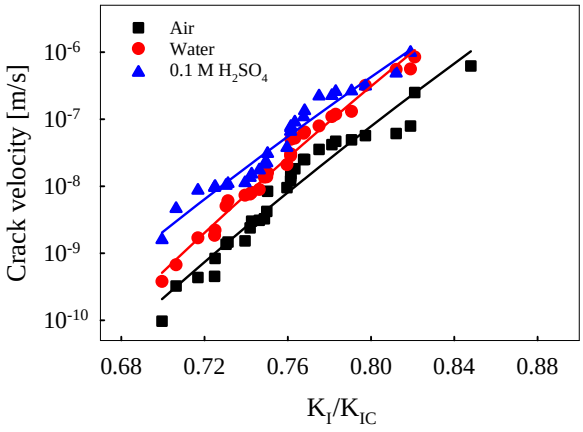

(a)

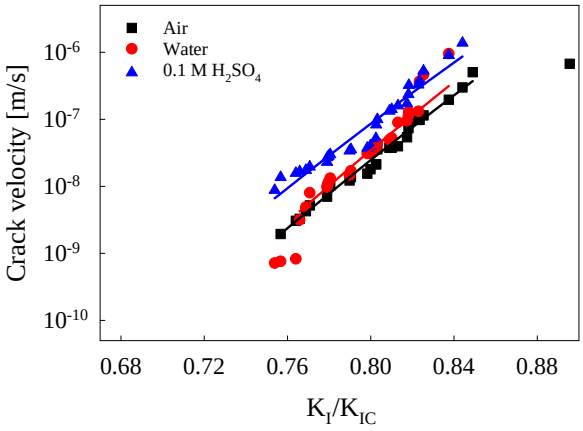

(b)

Figure 6: Subcritical crack growth rate of material A (a) and C (b) in air, water and 0.1 M H_2SO_4.

removing the three highest and lowest crack velocity values, a lower value of 48 was obtained. Although the n-values are different for the three materials the values may be regarded as similar within the uncertainty of the measurements as recently discussed by Krautgasser et al. [20].

The microstructure of fracture surfaces from the biaxial strength and subcritical crack growth experiments performed in air of material A and C is shown in Fig. 7. A transgranular fracture mode through the larger alumina grains is observed in all cases.

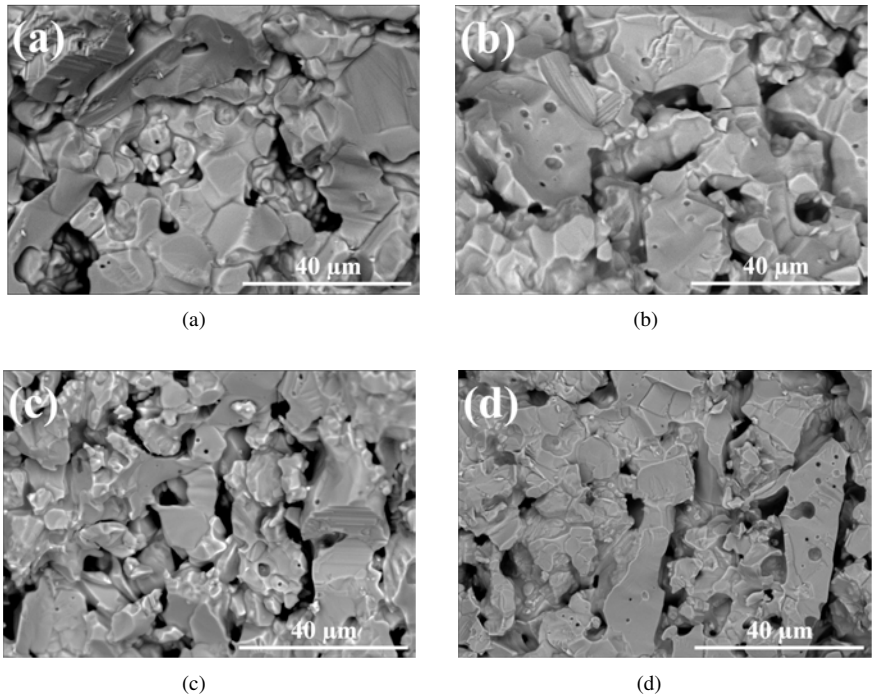

Figure 7: SEM images of transgranular fracture from measurements in air (a) material A after biaxial strength by BOR experiment and (b) material A after subcritical crack growth measurements by B3B method (c) material C after biaxial strength by BOR experiment and (d) material C after subcritical crack growth measurements by B3B method.

4. Discussion

The three materials investigated contained an increasing amount of silica sintering aid. The presence of silica together with the sodium impurities from the alumina powder results in the formation of a sodium aluminosilicate glass and an increasing amount of mullite with increasing silica content. The composition of the glass phase is different between alumina materials with or without the formation of mullite [29].

The biaxial strength obtained with the BOR technique were similar to the strength measured by the B3B method. ~~This was expected, since the specimens tested were relatively flat, with no apparent difference in thickness.~~ The similarity of the biaxial strength measured by the two methods can be rationalized by similar effective volume in the two tests. The thickness and surface of the specimens are the same and the influence of the similar surface may also result in comparable measured biaxial strength. When the support ring in the BOR technique is replaced with 3 touching spheres, the strength of slightly warped specimens can be obtained [15]. A higher strength was found for material A relative to material B, Table 2. The density and porosity of these two materials were similar and both materials demonstrated a transgranular fracture mode, see Fig. 7. ~~There are therefore no apparent simple explanation for the lower strength observed for material B.~~ The most significant difference between the two materials was the content of secondary phases. Only at the grain boundaries in material A a pure sodium aluminosilicate glassy phase was found, whereas crystalline mullite was present together with the glass at the grain boundaries in material B. The

composition of the glass phase is not the same in these two cases, since the liquid in equilibrium with only alumina or the combination of alumina and mullite are different [29]. The difference in the glass composition is one possible reason for the difference in biaxial strength. The presence of thermally induced stresses due to differences in thermal expansion of these materials may ~~could~~ influence the strength of the alumina~~, in form of reducing strength~~. The thermal expansion of the relevant materials are for alumina = 5-8.5 $\cdot 10^{-6}$ °C^{-1}[4], sodium aluminosilicate glass = 20-50 $\cdot 10^{-6}$ °C^{-1} [30] and mullite = 4.5 $\cdot 10^{-6}$ °C^{-1}[31]. Material C has the lowest strength measured by both the B3B and BOR test. The main reason for this is the higher degree of porosity compared to material A and B. In addition material C has the highest amount of crystalline mullite.

The rate of subcritical crack growth depends on chemical active species and stress at the crack tip. It has been reported that subcritical crack growth is promoted by water or water vapor in polycrystalline alumina [11, 18][14, 19–21]. The influence of water on the stress exponent in our experiments was minor compared to in air, however, a small decrease in the stress exponent was observed for the samples exposed to the acid. The crack growth rate of material A in air, water and acid was higher than compared to material C, which is indicated by a lower power law value for A in Table 2. The higher SCCG in acid is most likely related to the pH dependence of dissolution of the glass in water. The difference in SCCG in the two materials may relate to the residual stress due to the formation of mullite in material C, but this may also be related to the difference in the glass composition as discussed above. ~~The presence of a glassy sodium aluminosilicate phase without any mullite in material A, can promote subcritical crack growth.~~ It has been reported by Barinov et. al. [32] that glassy grain boundaries (Y_2O_3-Al_2O_3-SiO_2, 5wt%) in alumina ceramics promotes subcritical crack growth compared to Al_2O_3 (99.5 wt%, MgO) in both air and water. In acidic environment Al_2O_3 (99.5 wt%, MgO) was more susceptible towards subcritical crack growth compared to the yttria-glass bonded alumina [33].

The fracture mode found in these materials were transgranular mode with respect to the large alumina grains. SCCG is however related to the nature of the silica-rich grain boundary phase. The porosity and wide grain size distribution may therefore make it challenging to identify intergranular fracture, which would be influenced by subcritical crack growth in the grain boundary phase.

5. Conclusions

The biaxial strength, fracture toughness and subcritical crack growth of coarse grained porous alumina ceramics prepared using silica sintering aid are reported. The biaxial strength was shown to be influenced by the porosity and to some degree of the phase composition of the grain boundary region. At too high silica content formation of mullite will take place, which have an impact on the mechanical performance. The porous alumina was more susceptible to subcritical crack growth in water and acid relative to air, and the materials containing mullite in the glassy grain boundary phase displayed higher resistance towards subcritical crack propagation.

Acknowledgment

Funding provided by the Norwegian Research Council (NFR) and KeraNor AS is acknowledged (Nye materialer for bipolare batterier, NFR-193331). Travel grant received from Direktør Halvor B. Holtas legat at the Norwegian University of Science and Technology (NTNU).

References

[1] R. W. Rice, C. C. Wu, and F. Borchelt. Hardness grain-size relations in ceramics. *J. Am. Ceram. Soc.*, 77(10):2539–2553, 1994.
[2] P. S. Christel. Biocompatibility of surgical-grade dense polycrystalline alumina. *Clinical Orthopaedics and Related Research*, (282):10–18, 1992.
[3] R. L. Hentrich, G. A. Graves, H. G. Stein, and P. K. Bajpai. An evaluation of inert and resorbable ceramics for future clinical orthopedic applications. *J. Biomed. Mat. Res.*, 5(1):25–51, 1971.
[4] R. G. Munro. Evaluated material properties for a sintered alpha-alumina. *J. Am. Ceram. Soc.*, 80(8):1919–1928, 1997.
[5] W.D. Kingery, HK Bowen, and D.R. Uhlmann. *Introduction to ceramics*. John Wiley & Sons,Inc, 2 edition, 1975.
[6] K. A. Berry and M. P. Harmer. Effect of MgO solute on microstructure development in Al_2O_3. *J. Am. Ceram. Soc.*, 69(2):143–149, 1986.
[7] S. J. Bennison and M. P. Harmer. Grain-growth kinetics for alumina in the absence of a liquid-phase. *J. Am. Ceram. Soc.*, 68(1):C22–C24, 1985.

[8] S. I. Bae and S. Baik. Critical concentration of MgO for the prevention of abnormal grain-growth in alumina. *J. Am. Ceram. Soc.*, 77(10):2499–2504, 1994.
[9] O. Lyckfeldt and J. M. F. Ferreira. Processing of porous ceramics by 'starch consolidation'. *J. Eur. Ceram. Soc.*, 18(2):131–140, 1998.
[10] C. Marquez-Alvarez, N. Zilkova, J. Perez-Pariente, and J. Cejka. Synthesis, characterization and catalytic applications of organized mesoporous aluminas. *Catal. Rev. Sci. Eng.*, 50(2):222–286, 2008.
[11] A. G. Evans. Method for evaluating time-dependent failure characteristics of brittle materials - and its application to polycrystalline alumina. *J. Mater. Sci.*, 7(10):1137–1146, 1972.
[12] T. Fett, D. Badenheim, R. Oberacker, K. Heiermann, and R. Nejma. Subcritical crack growth of Al_2O_3, determined by different methods. *J. Mater. Sci. Lett.*, 22(5):363–365, 2003.
[13] A.D. Norton, S. Falco, N. Young, J. Severs, and R.I. Todd. Microcantilever investigation of fracture toughness and subcritical crack growth on the scale of the microstructure in Al_2O_3. *J. Eur. Ceram. Soc.*, 35(16):4521–4533, 2015.
[14] A. Krell, E. Pippel, J. Woltersdorf, and W. Burger. Subcritical crack growth in Al_2O_3 with submicron grain size. *J. Eur. Ceram. Soc.*, 23(1):81–89, 2003.
[15] R. Danzer, A. Borger, P. Supancic, and M. A. R. Villanueva. A simple strength test for brittle discs. *Materialwiss. Werkstofftech.*, 34(5):490–498, 2003.
[16] Henning Dannheim, Ulrich Schmid, and Andreas Roosen. Lifetime prediction for mechanically stressed low temperature co-fired ceramics. *J. Eur. Ceram. Soc.*, 24(8):2187–2192, 2004.
[17] Robert Danzer, Tanja Lube, Peter Supancic, and Rajiv Damani. Fracture of ceramics. *Adv. Eng. Mater.*, 10(4):275–298, 2008.
[18] P. Zhu, Z. Q. Lin, G. L. Chen, and I. Kiyohiko. The predictions and applications of fatigue lifetime in alumina and zirconia ceramics. *Int. J. Fatigue*, 26(10):1109–1114, 2004.
[19] J. J. Kruzic, R. M. Cannon, and R. O. Ritchie. Effects of moisture on grain-boundary strength, fracture, and fatigue properties of alumina. *J. Am. Ceram. Soc.*, 88(8):2236–2245, 2005.
[20] Clemens Krautgasser, Robert Danzer, Peter Supancic, and Raul Bermejo. Influence of temperature and humidity on the strength of low temperature co-fired ceramics. *J. Eur. Ceram. Soc.*, 35(6):1823–1830, 2015.
[21] George D. Quinn and Jeffrey J. Swab. Fracture toughness of glasses as measured by the scf and sepb methods. *J. Eur. Ceram. Soc.*, 37(14):4243–4257, 2017.
[22] R. W. Rice. Effects of environment and temperature on ceramic tensile strength grain size relations. *J. Mat. Sci.*, 32(12):3071–3087, 1997.
[23] T. Fett and D. Munz. Determination of v-K_I curves by a modified evaluation of lifetime measurements in static bending tests. *J. Am. Ceram. Soc.*, 68(8):C213–C215, 1985.
[24] A. Borger, P. Supancic, and R. Danzer. The ball on three balls test for strength testing of brittle discs: stress distribution in the disc. *J. Eur. Ceram. Soc.*, 22(9-10):1425–1436, 2002.
[25] A. F. Kirstein and R. M. Woolley. Symmetrical bending of thin circular elastic plates on equally spaced point supports. *Journal of Research of the National Bureau of Standards Section C-Engineering and Instrumentation*, C 71(1):1–10, 1967.
[26] Waloddi Weibull. A statistical distribution function of wide applicability. *J. Appl. Mech.*, 18(3):293–297, 1951.
[27] ASTM Standard C1421 - 10, "Standard test methods for determination of fracture toughness of advanced ceramics at ambient temperature", ASTM International, West Conshohocken, Pennsylvania, doi:10.1520/C1421-10, 2011.
[28] D. A. Pinnow, L. G. Van Uitert, T. C. Rich, F. W. Ostermayer, and W. H. Grodkiewicz. Investigation of the soda aluminosilicate glass system for application to fiber optical waveguides. *Mater. Res. Bull.*, 10(2):133–146, 1975.
[29] E. M. Levin, C. R. Robbins, and H. F. McMurdie. *Phase diagrams for ceramists*, volume 1. Am. Ceram. Soc., Columbus, Ohio, 2 edition, 1964.
[30] R. A. Lange. Temperature independent thermal expansivities of sodium aluminosilicate melts between 713 and 1835 k. *Geochim. Cosmochim. Acta*, 60(24):4989–4996, 1996.
[31] R. Torrecillas, J. M. Calderon, J. S. Moya, M. J. Reece, C. K. L. Davies, C. Olagnon, and G. Fantozzi. Suitability of mullite for high temperature applications. *J. Eur. Ceram. Soc.*, 19(13-14):2519–2527, 1999.
[32] S. M. Barinov, L. V. Fateeva, N. V. Ivanov, S. V. Orlov, and V. J. Shevchenko. Effect of acidic environment on subcritical crack growth in alumina ceramics. *Scripta Mater.*, 38(6):975–980, 1997.
[33] S. M. Barinov, N. V. Ivanov, S. V. Orlov, and V. J. Shevchenko. Influence of environment on delayed failure of alumina ceramics. *J. Eur. Ceram. Soc.*, 18(14):2057–2063, 1998.